

Cross-Linked Bacterial Cellulose Networks Using Glyoxalization

Franck Quero^{1, 2}, Masaya Nogi³, Koon-Yang Lee⁴, Geert Vanden Poel⁵, Alexander Bismarck⁴, Athanasios Mantalaris⁴, Hiroyuki Yano³ and Stephen J. Eichhorn^{1, 2}*

¹Materials Science Centre, School of Materials, University of Manchester, Grosvenor Street, Manchester, M14 9PL, UK.

²The Northwest Composite Centre, University of Manchester, Paper Science Building, Sackville Street, Manchester, M14 9PL, UK.

³Research Institute for the Sustainable Humanosphere, Kyoto University, Uji, Kyoto 611-011, Japan.

⁴Polymer and Composites Engineering (PaCE) Group, Department of Chemical Engineering, Imperial College London, South Kensington Campus, London, SW7 2AZ, UK.

⁵DSM Resolve, Thermal Analysis Group, P.O. Box 18, 6160 MD Geleen, The Netherlands.

*s.j.eichhorn@manchester.ac.uk

Telephone: +44 (0)161 306 5982, Fax: +44 (0)161 306 3586

ABSTRACT

In this study we demonstrate that bacterial cellulose (BC) networks can be crosslinked via glyoxalization. Modified BC networks are found to not dissolve in a typical cellulose solvent comprising a DMAc/LiCl mixture, whereas unmodified BC networks readily dissolve. The crystal structure of unmodified BC networks was investigated and found to not significantly change after glyoxalization, indicating heterogeneous modification occurs. No significant difference in moisture

content between unmodified and glyoxalized BC networks is found using thermogravimetric analysis. However the onset of degradation and the peak temperature is found to be significantly reduced after glyoxalization. Contact angle and zeta potential measurements confirm the hydrophobic nature of glyoxalized BC networks. Water absorption capacity shows that unmodified BC networks have a higher absorption capacity than glyoxalized BC networks, thus revealing their higher moisture resistance. Fracture surfaces of samples shows that, in the dry state, less delamination occurs for glyoxalized BC networks compared to unmodified BC networks, suggesting that covalent bond coupling between BC layers occurs during the glyoxylation process. In the wet state, glyoxalized BC networks experience significant delamination, but the layered structure is preserved. Young's moduli of dry unmodified BC networks do not change significantly after glyoxalization. The stress and strain at failure are however dramatically reduced after glyoxylation. The wet mechanical properties of the BC networks are also improved by glyoxylation. Raman spectroscopy is used to demonstrate that the stress-transfer of deformed dry and wet glyoxalized BC networks is significantly increased compared to unmodified material. This enhanced stress-transfer within the networks is shown to be as a consequence of the covalent coupling induced during glyoxylisation, and offers a facile route for enhancing the mechanical properties of BC networks for a variety of applications.

KEYWORDS Raman spectroscopy, bacterial cellulose, glyoxal, cross-linking, stress-transfer.

Introduction

Cellulose is the most abundant and utilized polymer on earth. It is found in higher plants, algae and is produced, under culturing conditions by bacteria^{1, 2}, and by sea animals called tunicates^{1, 2}. Bacterial cellulose (BC) is an extra-cellular product of bacteria identified for the first time by Brown^{3, 4}. Several families of bacteria are cellulose producers, namely, *Acetobacter*, *Entrobacter*, *Rhizobium*, *Agrobacterium*, and *Sarcina*⁵. The acetic acid bacteria *Acetobacter xylinum* (reclassified as *Gluconacetobacter xylinum*) have been found to be one of the most productive⁶ and consequently are

the most studied species. This form of BC is produced in a very pure form. Contrary to cellulose from plants, BC is free of wax, hemicellulose and lignin⁷.

Cellulose has been found to have desirable mechanical properties and is consequently a good candidate as a reinforcement in composite materials⁸⁻¹³. In plants, it naturally plays a structural role owing to its high stiffness. The crystal modulus of cellulose has been found to be ~138 GPa using X-ray diffraction^{14, 15}. More recently Young's modulus of single tunicate whiskers and BC nanofibers have been estimated using Raman spectroscopy; values of 143 GPa² and 114 GPa¹⁶ were found respectively. Another estimation, using an AFM cantilever method, yielded a value of 78 ± 17 GPa for BC nanofibrils¹⁷.

BC fibrous networks produced using different culturing times have been used to reinforce poly(L-lactic acid) (PLLA)¹⁸. Observations of the fracture surfaces of samples deformed in tension indicated that delamination occurred mainly between layers within the BC networks, rather than at the interface between the BC and PLLA. It was also found that the more layered the structure of these networks, the lower the stress-transfer efficiency. These layers in BC networks have been recently reported to be weakly linked¹⁹. Consequently in order to improve the stress-transfer efficiency of BC networks, we have crosslinked the material using glyoxal. We report the influence of this facile treatment on the mechanical and stress-transfer properties in both the dry and wet states.

It is possible to functionalize cellulose owing to the presence of a large number of accessible hydroxyl groups along its backbone structure. These hydroxyl groups can be functionalized via esterification¹³, polycondensation, etherification or acetalization reactions²⁰, to name a few. By using an appropriate chemical substance having at least two reactive groups that can react with hydroxyl groups, covalent bonds can be formed between cellulose polymer chains, and therefore potentially between weakly linked BC layers. Several chemical substances have been reported as cross-linking agents for cellulose; namely glyoxal and its homologues, but also formaldehyde, epichlorohydrin, epoxides (1,2,3,4-diepoxybutane), dichloroethane or diisocyanate²⁰. Most of these chemicals are not environmentally friendly, and/or toxic. Glyoxal is however an almost fully biodegradable and low

toxicity chemical (compared to formaldehyde), and can be obtained from renewable resources²¹ by the oxidation of lipids and as a by-product of biological processes²². Consequently this molecule is a good candidate to be used as an environmentally friendly cross-linker for cellulose. The main application of glyoxal thus far has been in the textile industry to impart durable wet mechanical properties of cotton fabrics²³. No application of glyoxal has, to the authors' knowledge, been proposed for cross-linking BC networks. When cellulose is exposed to water, its intra and intermolecular hydrogen bonding is disturbed leading to a dramatic decrease of the mechanical and stress-transfer properties. By cross-linking cellulose polymer chains with covalent bonds through glyoxalization, the effect of this disruption of hydrogen bonding on physical properties can be reduced. We show, for the first time, the potential of glyoxal to enhance the stress-transfer efficiency of BC networks, and thereby their mechanical properties. This modification is shown to persist in the wet state, and so could be used for a variety of applications; for example in composites manufacturing and biomedical applications.

Experimental Methods

Materials and chemicals *Gluconacetobacter xylinum* (no. 13693; National Institute of Technology and Evaluation, Tokyo, Japan) and Hestrin-Schramm (HS)²⁴ medium were used to produce BC networks. The cells for the inoculum were cultured in test tubes statically at 27 °C for 2 weeks. The thick gel produced during culturing was then squeezed aseptically to remove the embedded cells. The cell suspension (25 ml) was then transferred as an inoculum for the main culture (500 ml of medium), which was incubated statically at 27 °C for 14 days. BC networks (35 mm in diameter) were purified by boiling with 2% NaOH for 2 h, and then by washing with distilled water, followed by hot pressing at 2 MPa and 120 °C for 4 min to completely remove the bulk water.

Glyoxal (~40 wt. % in de-ionised water), aluminium sulfate hexadecahydrate ($\text{Al}_2 (\text{SO}_4)_3 \cdot 16 \text{H}_2\text{O}$, purity $\geq 98\%$), lithium chloride (LiCl; $\geq 99.5\%$) and N,N-dimethylacetamide (DMAc; $\geq 98\%$) were purchased from Sigma-Aldrich.

Glyoxal treatment of BC networks A solution of 5 wt. % of glyoxal was prepared by diluting a commercial glyoxal solution (40 wt. %) with de-ionised water. Aluminum sulfate was added with a concentration of 1 g.L⁻¹ to catalyze the reaction. The solution was agitated under mechanical stirring until complete dissolution of the catalyst. Narrow strips of BC (~ 30×1×0.060 mm) were immersed in the glyoxal solution for 5 hours. During that time the glyoxal molecules adsorbed on the surface and impregnated the structure of BC networks. These impregnated strips were then removed from the solution and placed in a convection oven at 150 °C for 15 minutes for glyoxalization to complete. Modified BC networks were then washed in de-ionised water at ~70 °C for four 15 minutes extractions. For each of these steps de-ionised water was renewed. The networks were dried overnight at 110 °C.

Dissolution test Strips of unmodified and glyoxalized BC samples (~ 2.5×1×0.060 mm) were immersed in LiCl/DMAc solution for 2 months in an environmentally controlled room at a temperature of 23 ± 1 °C and relative humidity of 50 ± 0.5 %. This solvent is reported to fully dissolve cellulose at room temperature. The glyoxalized samples were weighed before and after immersion in LiCl/DMAc solution using a Mettler Toledo AB265-S/FACT version classic analytical balance. Care was taken to remove the excess of LiCl/DMAc before weighing the samples. The percentage of swelling (%S) was determined after 48 hours using the equation

$$\%S = \frac{W_s - W_d}{W_d} \times 100 \quad (1)$$

where W_s and W_d are the swollen and dry weights of the glyoxalized BC networks respectively. Five samples were tested in total.

X-ray diffraction The degree of crystallinity and crystal morphology of unmodified and glyoxalized BC networks were determined using an X-ray powder diffractometer (Philips X'Pert 1) having a 1.79 Å cobalt X-ray source. Measurements were taken in the range $2\theta = 10^\circ$ to 40° using a step size of 0.04° . Five samples were analysed for both unmodified and glyoxalised BC networks. In order to calculate the percentage crystallinity ($\% \chi_c$) of BC, Segal's method²⁵ was utilized. This method uses the equation

$$\% \chi_c = \frac{I_{002} - I_{\text{amorphous}}}{I_{002}} \times 100 \quad (2)$$

to calculate the percentage crystallinity, where I_{002} is the intensity of the 002 reflection plane and $I_{\text{amorphous}}$ is the intensity of the amorphous phase at 18° , if a copper X-ray source is used. For a cobalt source the intensity at 21° is recorded. For the lateral crystal size ($L_{(002)}$) determination, Scherrer's equation

$$L_{(002)} = \frac{K\lambda}{\beta \cdot \cos \theta} \quad (3)$$

was used, where β is the full width at half maximum of the 002 reflection, θ is the Bragg angle and a value of $K = 0.91$ was used.

Thermogravimetric analysis The thermal degradation behavior of unmodified and glyoxalized BC was investigated using thermogravimetric analysis (TGA Netzsch TG 209 F1). The samples (approximately 5 mg) were heated from 25 to 600°C at a heating rate of 5°C min^{-1} under a flow of 30 mL min^{-1} nitrogen purge gas. Experiments were repeated three times to ensure repeatability. The onset

and degradation temperatures were obtained from the first derivative of the loss weight as a function of temperature.

Water/air contact angle measurements Advancing and receding contact angles were measured on unmodified and glyoxalized BC networks using a sessile drop method (DSA 10 Mk 2, Krüss) at room temperature. Droplets of approximately 20 μL of ultra pure water were placed on the surface of unmodified and glyoxalized BC networks using a motorized syringe and the drop volume was increased at a rate of 6.32 $\mu\text{L min}^{-1}$. Images of these sessile drops were processed using DSA software version 1.80.1.12. Measurements were repeated at 5 different positions on the samples.

Streaming zeta-potential measurements The zeta-potentials of unmodified and glyoxalized BC were measured using an electrokinetic analyser (EKA, Anton Paar) based on a streaming potential method. In order to exclude any overlaying effects, due to the swelling of unmodified and glyoxalized BC networks or extraction of water-soluble components, the pH dependent zeta-potentials were measured after a time dependent measurement was conducted. During the time dependent measurements, the samples were equilibrated in 1 mM KCl electrolyte solution by means of a single long time streaming zeta-potential measurement at 20°C. A pH-dependent zeta-potential measurement was then conducted by changing the pH of the electrolyte solution via the titration of 0.1 N HCl or KOH, using a titration unit (RTU, Anton Paar). The swelling behaviour was also determined from the kinetic parameters ζ_0 (initial zeta potential at first contact with water) and ζ_∞ (final zeta potential, asymptotic approach). The relative change in the zeta-potential was found using the equation

$$\Delta\xi = \frac{\xi_0 - \xi_\infty}{\xi_0} \quad (4)$$

It was found that this quotient is proportional to the water uptake at 100% relative humidity (the sorption capacity) of natural fibres.

Water absorption capacity Unmodified and glyoxalized BC networks ($\sim 5 \times 1 \times 0.060$ mm) were conditioned for 7 days at 23 ± 1 °C and a relative humidity of 50 ± 0.5 % and immersed in de-ionised water for 48 hours. The samples were weighed after 2, 5, 11, 24 and 48 hours using a top pan balance. Care was taken to remove excess water before weighing the samples. Water absorption capacity (%*WAC*) was determined using the equation

$$\%WAC = \frac{w_t - w_{t_0}}{w_{t_0}} \times 100 \quad (4)$$

where w_{t_0} and w_t are the weights of the samples before and after water immersion respectively. Five samples were tested for each material.

Mechanical properties Unmodified and glyoxalized BC strips ($\sim 20 \times 1 \times 0.060$ mm) were secured to 20 mm gauge length testing cards using a two-part cold curing epoxy resin (Araldite®). Tensile tests were conducted using a tensile testing machine (Instron 2511-111). The full-scale load and the crosshead speed used were 50 N and 0.5 mm min^{-1} respectively. The machine compliance was determined and found to be $4.42 \times 10^{-3} \text{ mm N}^{-1}$. All mechanical data were adjusted to take into account the machine compliance. Dry and wet mechanical tests were conducted at 23 ± 1 °C and a relative humidity of 50 ± 0.5 %. The samples were pre-conditioned under the same environmental conditions for

24 hours prior to testing. A total of 10 samples were tested for each material. Sample widths and thicknesses were determined using an optical microscope and a micrometer, respectively.

For wet mechanical properties determination, unmodified and glyoxalized BC networks were immersed in de-ionised water for 48 hours using the previously stated environmental conditions. The samples were then removed from the water and secured on paper testing cards using cyanoacrylate glue.

The fracture surfaces of dry and wet unmodified and glyoxalized BC networks deformed in tension were observed using a scanning electron microscope (FEG-SEM). The acceleration voltage used was 5 kV. Prior to SEM imaging, the samples were fixed onto metal stubs using carbon tabs and gold coated at 40 mA for 2 min.

Raman spectroscopy In order to follow the molecular deformation of unmodified and glyoxalized BC networks a Raman spectrometer (Renishaw system-1000) coupled with an optical microscope and a near infra-red laser (785 nm) was used. The laser was focussed to a 1-2 μm spot using a $\times 50$ magnification long working distance lens. Dry unmodified and glyoxalised BC strips were mounted on paper testing cards using a two-part cold-curing epoxy resin (Araldite[®]). The samples were deformed in tension using a customized deformation rig (Deben Microtest). The compliance of the deformation rig was determined to be $3.14 \times 10^{-4} \text{ mm N}^{-1}$. All mechanical data were adjusted to take into account the machine compliance. The gauge length of the samples and the full scale of the load cell used were 20 mm and 2 kN respectively. During the deformation, the strain was increased incrementally by 0.025 % and then 0.1 % at an elongation rate of $0.033 \text{ mm min}^{-1}$. A Raman spectrum was recorded at each increment using an exposure time of 30 s and 4 accumulations. The peak positions of the Raman band initially located at approximately 1095 cm^{-1} were fitted using a mixed Gaussian/Lorentzian function and an algorithm suggested by Marquardt²⁶. Experiments were repeated 3 times for unmodified and glyoxalized BC networks.

The molecular deformation of samples in the wet state was also investigated. Unmodified and glyoxalized BC networks were immersed in de-ionised water for 48 hours. The samples were then removed from the water and secured on paper testing cards using cyanoacrylate glue. During sample preparation and molecular deformation the BC networks were regularly wetted. Two samples were tested for each material.

Results and discussion

Glyoxal can react with the hydroxyl groups of cellulose either by an acetalization reaction or by glyoxalization²⁷. They can form either or both acetal and hemiacetal linkages during the curing process²⁸. In order to check if cross-linking occurred, unmodified and glyoxalized samples were immersed in LiCl/DMAc for 2 months. Unmodified BC samples were found to be fully dissolved after 24 hours whereas glyoxalized BC samples did not dissolve, but were in a swollen state. After 48 hours, the percentage of swelling was found to be 30 ± 4 %. Since dissolution of the glyoxalized BC networks did not take place, it is very likely that cross-linking occurs between BC layers after this treatment. This dissolution method has been already used to assess the extent of cross-linking in chemically modified cotton, with cuprammonium hydroxide as a solvent²⁹.

Figure 1 reports typical X-ray diffraction patterns for dry unmodified and glyoxalized BC networks. It can be seen that the crystal structure is unchanged after glyoxalization since (101), $(10\bar{1})$ and (002) diffraction planes are still observed. Table 1 reports percentage crystallinity values and crystal dimensions for dry unmodified and glyoxalized BC networks. No significant difference between dry unmodified and glyoxalized BC networks is observed. This result suggests that cross-linking is likely to occur only at the surface of BC fibrils, and in amorphous regions, meaning that heterogeneous modification of BC has occurred. Hydroxyl groups located inside crystal regions are believed to be inaccessible to chemical modification³⁰.

Figure 2 reports the thermal degradation behavior for unmodified and glyoxalized BC networks. The thermal behavior indicates that cross-linking has occurred, since a higher onset and peak

degradation temperature is observed. An initial weight loss was observed in the temperature range of 0 to 200 °C, which is due to water loss. No significant differences between unmodified and glyoxalized BC networks were observed in this region, indicating that there is no difference in moisture content between these samples (see insert). This means that if a change of mechanical or stress-transfer properties is observed in the dry state, it should be due only to the presence of cross-linking, and not from a plastification effect due to the presence of moisture. A second weight loss is visible from 200 to 375 °C which is attributed to the degradation of cellulose. Table 2 reports the onset and peak degradation temperatures for unmodified and glyoxalized BC networks. In agreement with previous reports^{31, 32}, there is only a slight decrease in the onset and peak degradation temperatures after glyoxalization, meaning that this process does not dramatically decrease thermal stability.

Glyoxal has been previously found to render chitosan hydrophobic³³. This suggests that it ought to be possible to also render BC networks hydrophobic. Therefore water/air contact angle measurements were conducted. Advancing contact angles were found to be $17.41 \pm 1.74^\circ$ and $29.59 \pm 1.79^\circ$ for unmodified and glyoxalized BC networks respectively. A receding contact angle of $9.93 \pm 0.64^\circ$ was also measured for glyoxalized BC networks. We could not measure the receding value for unmodified BC networks since the material wetted before a measurement could be made, but it is likely to be low. These results suggest a mild increase in the hydrophobicity of the BC networks, but not to the same extent as seen for chitosan³³.

Figure 3 shows the streaming zeta-potential of unmodified and glyoxalized BC as a function of pH. The negative zeta-potential plateau and isoelectric point (iep) at acidic pH indicate that the surface of unmodified and glyoxalized BC networks are acidic. In addition to this, the zeta-potential plateau for glyoxalized BC networks was shifted to more negative value, indicating that its surface is more hydrophobic than the unmodified BC networks. The hydrophobic surface of glyoxalized BC (also confirmed by contact angle measurements) would lead to more adsorption by electrolyte ions compared to unmodified BC, as water molecules cannot as readily adsorb due to the hydrophobic nature of the surface of glyoxalized BC networks. A shift in the iep of glyoxilized BC to lower pH was also observed.

This might be due to the fact that the glyoxilization reaction introduced more free acidic functional groups to the surface. More dissociable acidic functional groups implies lower iep . We also calculated $\Delta\zeta$ from $\zeta=f(t)$ for unmodified and glyoxalized BC networks (see figure 3b). Values of 0.255 and 0.184 were found for unmodified BC and glyoxalized BC, respectively. The higher value of $\Delta\zeta$ indicates that unmodified BC networks have a higher water absorption capacity compared to glyoxalized BC networks. This is not surprising due to the hydrophilic nature of unmodified BC.

Figure 4 reports water absorption as a function of time for unmodified BC and glyoxalized BC. After two hours unmodified and glyoxalized BC networks were saturated with water; no significant changes were observed after 5, 12, 24 and 48 hours. A significant difference between the relative water absorption capacities of unmodified and glyoxalized BC networks is however noted; unmodified BC is much higher than glyoxalized BC. This result is consistent with the calculation of the variation of zeta-potential (the lower that variation, the lower the water absorption capability) and with the contact angle and zeta-potential measurements since a more hydrophobic surface will absorb less water than a more hydrophilic one. Hence the presence of cross-linking must also reduce the swelling of BC networks with water. This reduced water absorption capacity has also been observed for biodegradable plastics made from soy bean products cross-linked with glyoxal³³. This difference in water absorption capacity will have to be taken into account when interpreting the stress-transfer and mechanical properties in the wet state. This result is also interesting because moisture resistance is often an issue for cellulose-based biocomposites. The use of glyoxalised BC networks could therefore help to produce biocomposites with enhanced moisture/swelling resistance.

Figures 5a and 5b show scanning electron microscopy images of the fracture surfaces of dry unmodified and glyoxalized BC networks deformed in tension. Clear delamination of BC layers is observed for the unmodified networks. BC fibrils can also be seen bridging these delaminated layers which must play a role in the fracture process. Such a delamination process does not occur for dry glyoxalised BC networks, which must be due to the presence of chemical cross-linking between layers. Figure 5c reports scanning electron microscope images for unmodified BC samples fractured whilst wet

(the samples are dry within the vacuum chamber of the SEM). The cross-sections of the samples appear to be considerably reduced compared to the dry samples, and we did not observe any delamination of the layers. Some kind of plastification effect (see arrows) is however observed. Figure 5d reports a scanning electron microscopy image for the tensile fracture surface of a wet glyoxalized BC network. These samples were found to maintain their dimensions, not reducing in thickness. Delamination of BC layers is however observed for this sample.

Figure 6 reports typical stress-strain curves for dry and wet unmodified and glyoxalized BC networks. The mechanical properties of dry unmodified and glyoxalized BC networks are also reported in Table 3. In the dry state, one can clearly see that glyoxalization of the samples reduces stress and strain at failure, and the work of fracture, indicating an embrittlement of the material. Indeed this embrittlement is matched by the clean fracture surfaces observed for glyoxalized BC networks (see Fig. 5b). This embrittlement may occur due the presence of cross-linking between BC layers, which will reduce layer-to-layer mobility, and consequently delamination. Cross-linking must also occur in the plane of the specimen, which could reduce orientation effects previously reported for BC networks³⁴. No difference between Young's modulus of unmodified and glyoxalized BC networks was however observed, suggesting little difference in the cross-linking in the longitudinal direction. The transverse mechanical properties could be significantly different, due to cross-linking between layers in the BC network, but that remains a topic for future work. It is also possible that there could be a decrease of the molecular weight of the BC networks upon glyoxalization. However we would require more evidence to support this hypothesis.

When the BC networks are in the wet state, a large decrease of Young's modulus and stress at failure occurs. An increase in the strain at failure for wet unmodified BC networks compared to dry unmodified BC networks also occurs. Young's modulus, stress at failure and strain at failure change by 438, 1570 and 261 % respectively, when samples are in the wet state. These large significant changes could be explained by the disruption of hydrogen bonding by competitive binding of water molecules, allowing slippage between BC fibrils. The modulus of wet glyoxalized BC networks is reduced by 77 %,

compared to the dry state. The stress at failure does not change significantly, but the strain at failure is increased by 137 %. The presence of crosslinks which prevent cellulose polymer chains from slipping from one another is therefore thought to maintain the strength of the networks.

Figure 7a reports typical Raman spectra for unmodified and glyoxalized BC networks. We did not observe any difference between spectra which suggests that the cellulose backbone has not been affected by chemical modification, which also confirms that heterogeneous modification has occurred. The Raman band initially located at 1095 cm^{-1} , highlighted in Figure 7a, has been extensively used for stress-transfer quantification in cellulose materials^{1, 17, 15, 34}. This band is thought to be representative of C-O ring stretching modes³⁵ and/or the C-O-C glycosidic bond stretching^{36, 37}.

Figures 7b and 7c report typical shifts in the position of the Raman band initially located at 1095 cm^{-1} for dry unmodified and glyoxalized BC networks respectively. It was noted that the shift in this band is higher in magnitude for dry networks compared to wet samples, in agreement with previous work on wet cellulose nanowhisker-based composite materials³⁸. Figure 8a reports the detailed positions of the Raman band initially located at 1095 cm^{-1} as a function of strain for dry unmodified and glyoxalized BC networks. The stress-transfer efficiency of the networks can be obtained from the gradient of a linear fit to these data. A higher stress-transfer efficiency is observed for glyoxalised BC networks compared to unmodified samples, which is an indication of the cross-linking that has taken place. The gradient of these linear fits for dry unmodified and glyoxalized BC networks were $-0.85 \pm 0.13\text{ cm}^{-1}\text{ \%}^{-1}$ and $-1.66 \pm 0.05\text{ cm}^{-1}\text{ \%}^{-1}$ respectively. As previously noted, less delamination occurred for glyoxalized BC networks, which is thought to contribute to the higher stress-transfer efficiency. As a consequence of this, less energy is likely to be dissipated throughout the structure. This is confirmed by the higher work of fracture for dry unmodified BC networks compared to glyoxalized BC networks (Table 3).

Figure 8b reports the wet stress transfer properties of the networks, as revealed by the shift in the position of the Raman band located at 1095 cm^{-1} . It is clear that the presence of water within unmodified BC networks almost completely suppresses their stress-transfer efficiency. This effect has also been observed for cellulose whisker-based nanocomposites exposed to water³⁴. This suggests that water has

fully penetrated the BC networks, and therefore acts as a plasticizer, disrupting hydrogen bonding between fibrils, and consequently reducing local molecular deformation and therefore stress-transfer within the network. The stress-transfer efficiency of wet glyoxalized BC networks is however preserved by cross-linking; the linear fit to these data was found to be $1.32 \text{ cm}^{-1}\%^{-1}$, which is only slightly lower than for dry glyoxalized BC networks ($1.66 \text{ cm}^{-1} \text{ \%}^{-1}$). This explains why the mechanical properties of glyoxalized BC networks, particularly strength, were hardly affected by the presence of water (see Table 3). Differences in the stress-transfer efficiencies of dry and wet glyoxalized BC networks must be due to the removal of hydrogen bonding after immersion in water. Water absorption experiments showed that glyoxalized BC networks absorb much less water than unmodified BC networks, and so this might also explain why stress-transfer is preserved for wet glyoxalized BC networks.

Conclusions

This study has shown that it is possible to crosslink BC networks via glyoxalization. The glyoxalization process was found to not significantly change the degree of crystallinity and crystal morphology of the BC, meaning that heterogeneous modification of cellulose occurred. Thermogravimetric analysis showed that the onset and peak degradation temperatures were significantly reduced after glyoxalization. Contact angle and zeta-potential measurements showed that glyoxal rendered the BC networks hydrophobic. In the dry state, Young's modulus was found not to be significantly changed after glyoxalization. Stress and strain at failure, and work of fracture, were found to however reduce upon modification. The reduced work of fracture values were supported by tensile fracture surface observations using scanning electron microscopy, suggesting that delamination of the layered structure of glyoxalized BC networks also reduced, owing to the presence of cross-linking. In the wet state, the mechanical properties of unmodified BC networks were reduced due to the disruption of hydrogen bonding. The mechanical properties, particularly the strength, of wet glyoxalized BC networks did not however reduce, compared to the dry state, again due to the presence of cross-linking. This was also supported by scanning electron microscopy imaging. Consequently glyoxal cross-linking

offers dimensional and mechanical stability to the BC networks when exposed to moisture. Water absorption capacity experiments clearly showed that glyoxalized BC networks do not absorb as much water as unmodified BC networks. Zeta-potential measurements also confirmed this result. These findings could have implications for the design of biocomposites generated from BC with increased moisture resistance. Finally, Raman spectroscopy revealed the stress-transfer mechanisms of unmodified and glyoxalized BC networks both in the dry and wet states. Micromechanical characterization showed that glyoxalization of BC networks results in a higher stress-transfer efficiency. This was found to be also true in the wet state. This greater stress-transfer efficiency of glyoxalized BC networks is thought to be due to the presence of cross-linking, but also to difference in the relative water absorptions of the networks. The use of glyoxal therefore provides a facile approach to modify the stress-transfer properties of BC networks, which could be used for a range of applications.

Acknowledgements

The authors would like to thank the EPSRC for funding the PhD studentship under Grant GR/F028946 and EP/F032005/1. Thanks are extended to Dr. Henning Althoefer from BASF for useful advises.

References

1. Ranby, B. G. *Arkiv for Kemi* **1952**, 4, (3), 241-&.
2. Sturcova, A.; Davies, G. R.; Eichhorn, S. J. *Biomacromolecules* **2005**, 6, (2), 1055.
3. Brown, A. J. *Journal of Chemical Society* **1986**, (49), 172.
4. Brown, A. J. *Journal of Chemical Society* **1986**, (49), 432.
5. Jonas, R.; Farah, L. F. *Biodegradable Polymers and Macromolecules* **1998**, 59, (1-3), 101.
6. Keshk, S. M. A. S.; Razek, T. M. A.; Sameshima, K. *African Journal of Biotechnology* **2006**, 5, (17), 1519.
7. Nishi, Y.; Uryu, M.; Yamanaka, S.; Watanabe, K.; Kitamura, N.; Iguchi, M.; Mitsuhashi, S. *Journal of Materials Science* **1990**, 25, (6), 2997.
8. Kim, Y.; Jung, R.; Kim, H. S.; Jin, H. J. *Current Applied Physics* **2009**, 9, (1 SUPPL.), S69.
9. Gindl, W.; Keckes, J. *Composites Science and Technology* **2004**, 64, (15 SPEC. ISS.), 2407.
10. Huang, Y.; Wan, Y.; Hu, L.; He, F.; Wang, Y. *Fuhe Cailiao Xuebao/Acta Materiae Compositae Sinica* **2008**, 25, (6), 140.
11. Yano, H.; Sugiyama, J.; Nakagaito, A. N.; Nogi, M.; Matsuura, T.; Hikita, M.; Handa, K. *Advanced Materials* **2005**, 17, (2), 153-155.
12. Gea, S.; Torres, F. G.; Troncoso, O. P.; Reynolds, C. T.; Vilasecca, F.; Iguchi, M.; Peijs, T. *International Polymer Processing* **2007**, 22, (5), 497.
13. Lee, K.-Y.; Blaker, J. J.; Bismarck, A. *Composites Science and Technology*. **2009**.

14. Sakurada, I.; Nukushina, Y.; Ito, T. *Journal of Polymer Science* **1962**, 57, (165), 651-660.
15. Nishino, T.; Takano, K.; Nakamae, K. *Journal of Polymer Science Part B: Polymer Physics* **1995**, 33, (11), 1647-1651.
16. Hsieh, Y. C.; Yano, H.; Nogi, M.; Eichhorn, S. J. *Cellulose* **2008**, 15, (4), 507.
17. Guhados, G.; Wan, W.; Hutter, J. L. *Langmuir* **2005**, 21, (14), 6642.
18. Quero, F.; Nogi, M.; Yano, H.; Abdulsalami, K.; Holmes, S. M.; Sakakini, B. H.; Eichhorn, S. J. **2009**, 2, (1), 321.
19. Nogi, M.; Yano, H. *Advanced Materials* **2008**, 20, (10), 1849.
20. Klemm, D., Philipp B., Heinze T., Heinze U., Wagenknecht W. **1998**, 2.
21. Ramires, E. C.; Megiatto Jr, J. D.; Gardrat, C.; Castellán, A.; Frollini, E. 101, (6), 1998.
22. Miyata, T.; Kurokawa, K.; Van Ypersele De Strihou, C. *Journal of the American Society of Nephrology* **2000**, 11, (9), 1744.
23. Welch, C. M.; Forthright Danna, G. *Textile Research Journal* **1982**, 52, (2), 149.
24. Hestrin, S.; Schramm, M. *Biochem. J.* **1954**, 58, 345-352.
25. Segal, L., Creely, J.J., Martin, A.E., Jr, Conrad, C.M. *Textile Research Journal* **1959**, 29, 786-794.
26. Marquardt, D. W. *Society for Industrial and Applied Mathematics* **1963**, 11, (2), 431.
27. Head, F. S. H. *Journal of the Textile Institute Transactions* **1958**, 49, (7), 345 - 356.
28. Schramm, C.; Rinderer, B. **2000**, 72, (23), 5829.
29. Reeves, W. A.; Drake, G. L. J. R.; McMillan, O. J. J. R.; Guthrie, J. D. *Textile Research Journal* **1955**, 25, (1), 41.
30. Krassig. **1993**.
31. Lee, E.; Kim, S. *Fibers and Polymers* **2004**, 5, (3), 230.
32. Hyung-Min, C.; Jung Hyun, K.; Sangmoo, S. *Journal of Applied Polymer Science* **1999**, 73, (13), 2691-2699.
33. Gupta, K. C.; Jabrail, F. H. **2006**, 341, (6), 744.
34. McKenna, B. A.; Mikkelsen, D.; Wehr, J. B.; Gidley, M. J.; Menzies, N. W. *Cellulose* **2009**, 16, (6), 1047-1055.
35. Wiley, J. H.; Atalla, R. H. *Carbohydrate Research* **1987**, 160, 113-129.
36. Edwards, H. G. M.; Farwell, D. W.; Webster, D. *Spectrochimica Acta Part a-Molecular and Biomolecular Spectroscopy* **1997**, 53, (13), 2383-2392.
37. Gierlinger, N.; Schwanninger, M.; Reinecke, A.; Burgert, I. *Biomacromolecules* **2006**, 7, (7), 2077-2081.
38. Rusli, R.; Shanmuganathan, K.; Rowan, S. J.; Weder, C.; Eichhorn, S. J. *Biomacromolecules* **2010**, 11, (3), 762-768.

LIST OF TABLES

- Table 1** Percentage crystallinity (χ_c) and lateral crystal sizes (L) for dried unmodified and glyoxalized BC networks
- Table 2** Onset and peak degradation temperatures for unmodified and glyoxalized BC networks.
- Table 3** Mechanical properties for dry and wet unmodified and glyoxalized BC networks; E - Young's modulus, σ_f - stress at failure, ε_f - strain at failure and G - work-of-fracture.

LIST OF FIGURES

- Figure 1** Typical X-ray diffraction patterns for dry unmodified and glyoxalized BC networks.
- Figure 2** Typical thermal degradation profiles for unmodified and glyoxalized BC networks. Error bars are standard deviations from the mean. The insert represents the thermal behavior from 25 °C to 200 °C.
- Figure 3** (a) Streaming zeta-potentials of unmodified and glyoxilized BC as a function of pH.; (b) Streaming zeta-potentials of unmodified and glyoxilized BC as a function of time.
- Figure 4** Relative water absorption as a function of time for unmodified and glyoxalized BC.
- Figure 5** Scanning electron microscope images of fracture surfaces for dry (a) unmodified and (b) glyoxalized BC networks and wet (c) unmodified and (d) glyoxalized BC networks.
- Figure 6** Typical stress-strain curves for dry and wet unmodified and glyoxalized BC networks.
- Figure 7** (a) Typical Raman spectra for dry unmodified and glyoxalized BC networks; Typical shifts in the position of the Raman band initially located at 1095 cm^{-1} towards a lower wavenumber for a dry (b) unmodified BC network and (c) a glyoxalized BC network.
- Figure 8** Detailed typical shifts in the position of the Raman band located at 1095 cm^{-1} for (a) dry unmodified and glyoxalized BC networks and (b) wet unmodified and glyoxalized BC networks. Errors are standard deviations from the mean for 2 samples (BC1 and BC2)

Material	χ_c (%)	L (002) (Å)	d (002) (Å)
Unmodified BC	94.31 ± 1.21	62.97 ± 2.12	7.82 ± 0.05
Glyoxalized BC	93.85 ± 0.18	63.56 ± 0.47	7.85 ± 0.04

Table 1

Material	Onset degradation temperature (°C)	Peak degradation temperature (°C)
Unmodified BC	319.00 ± 1.12	334.58 ± 3.82
Glyoxalized BC	299.30 ± 0.78	329.58 ± 2.89

Table 2

Material	E (GPa)	σ_f (MPa)	ϵ_f (%)	G (MJ m ⁻³)
Dry unmodified BC	10.12 ± 1.53	165.14 ± 33.86	2.57 ± 0.63	2.52 ± 0.90
Dry glyoxalized BC	10.67 ± 1.36	71.04 ± 36.04	0.64 ± 0.32	0.26 ± 0.24
Wet unmodified BC	1.88 ± 0.24	9.89 ± 1.47	9.28 ± 1.86	5.18 ± 0.62
Wet glyoxalized BC	6.04 ± 1.41	76.82 ± 21.23	1.52 ± 0.66	1.29 ± 0.84

Table 3

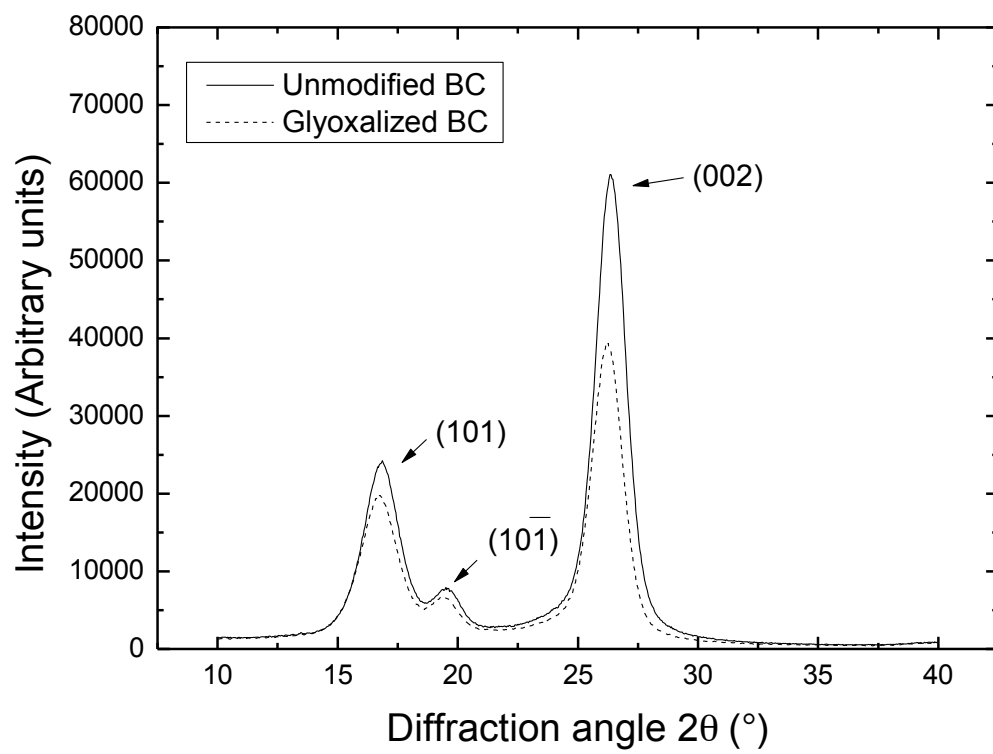


Figure 1

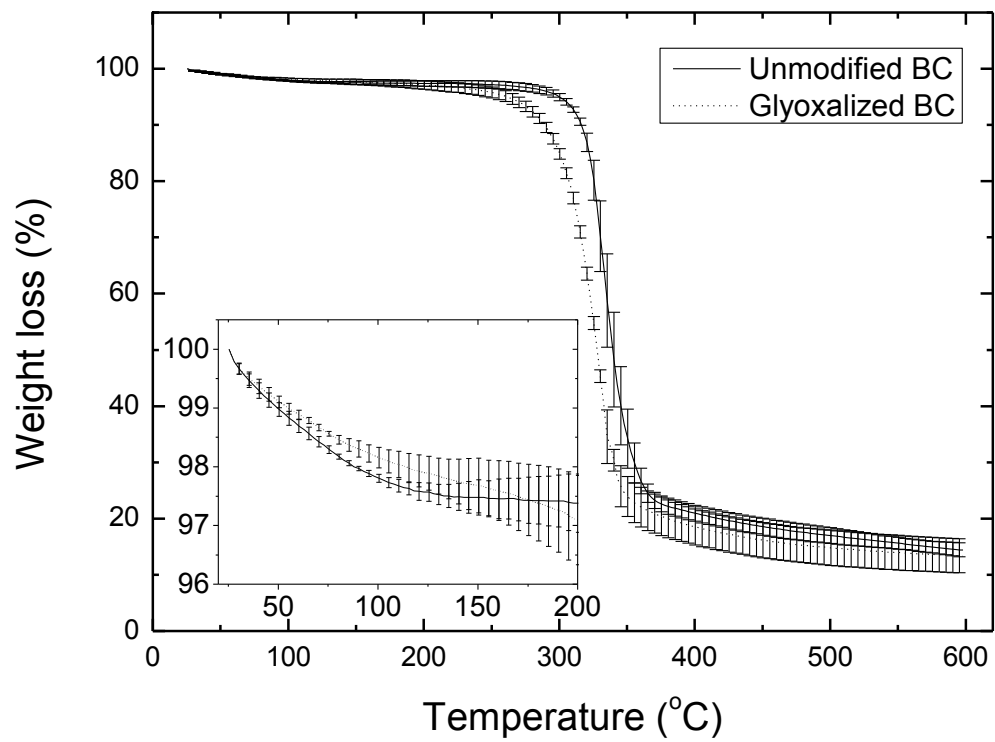
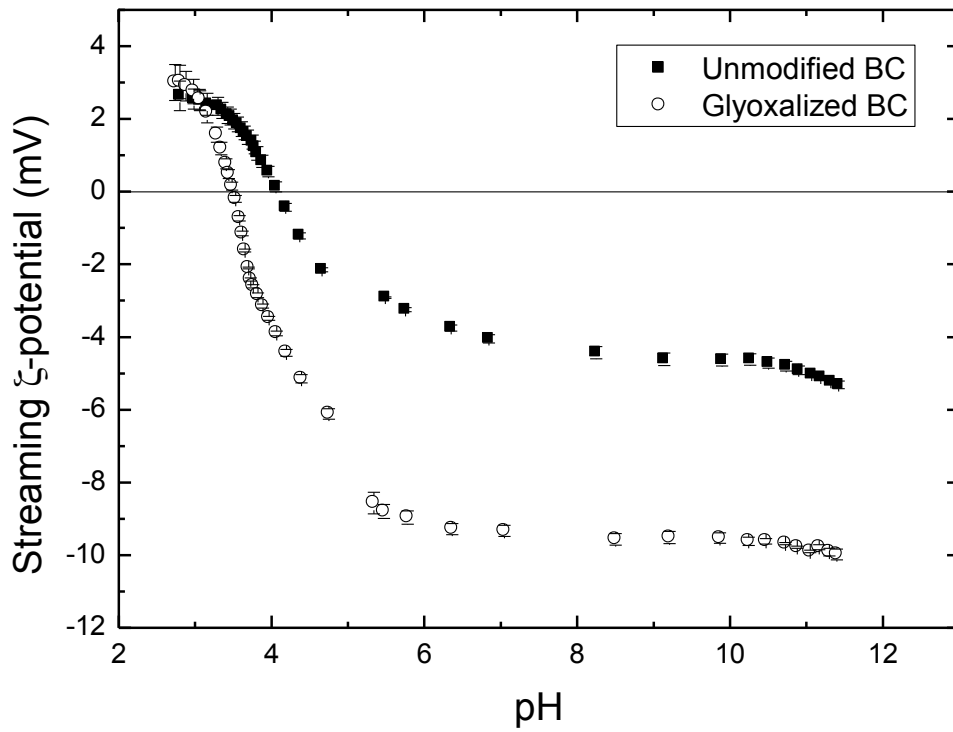


Figure 2

(a)



(b)

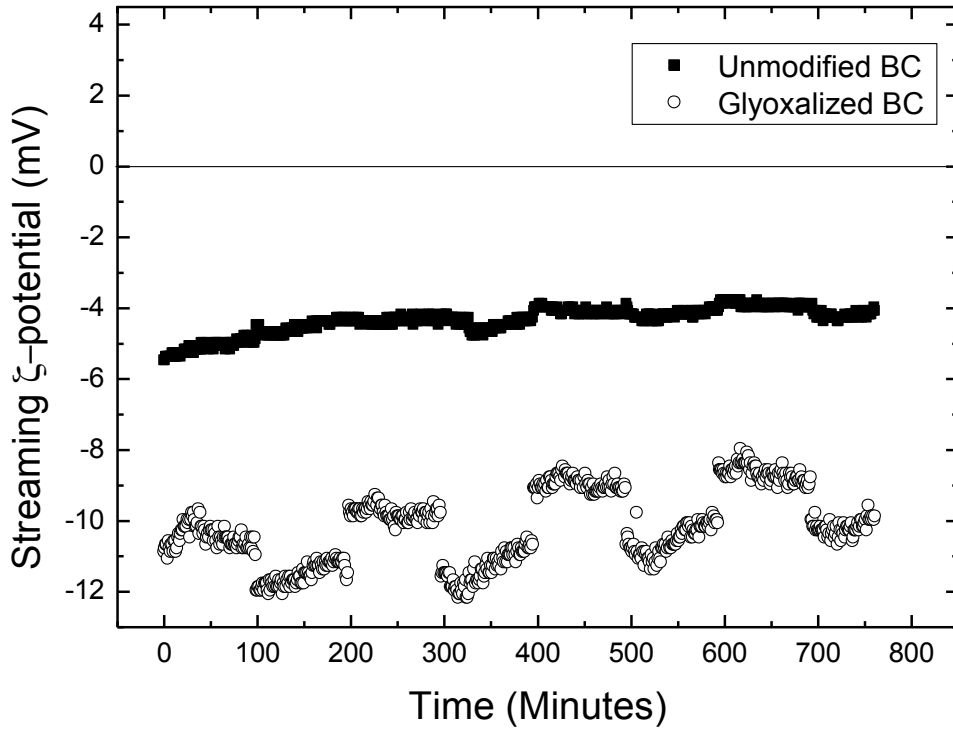


Figure 3

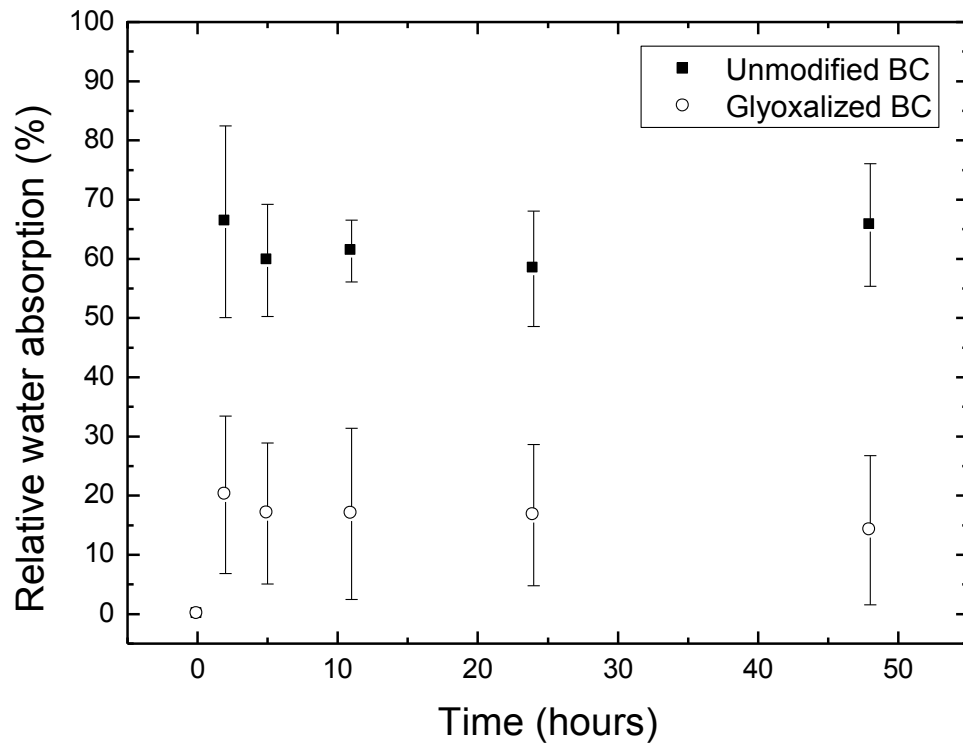
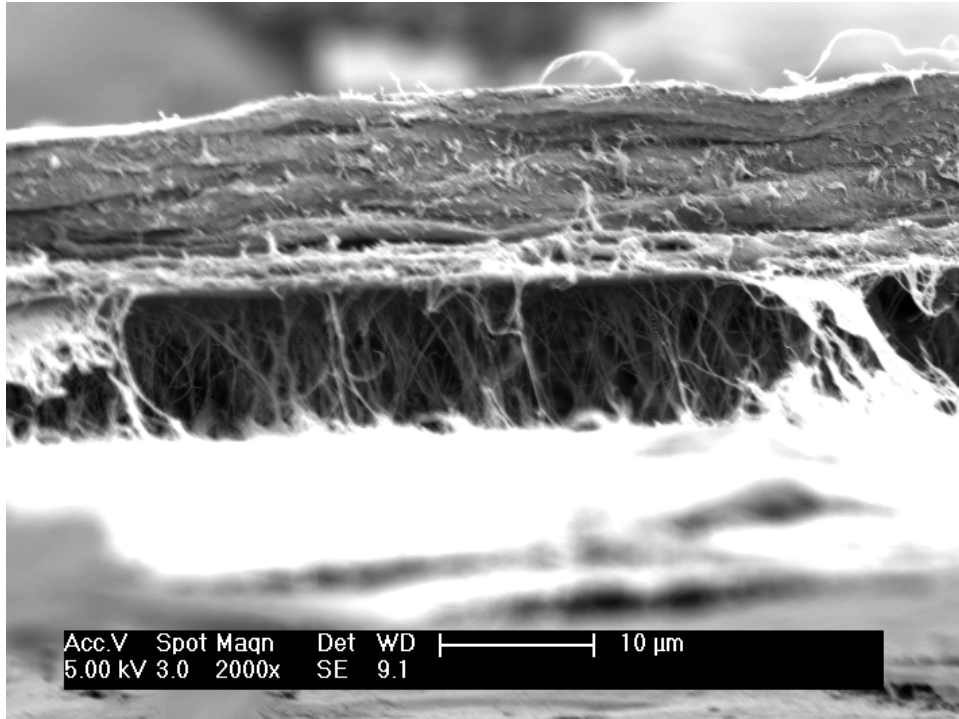
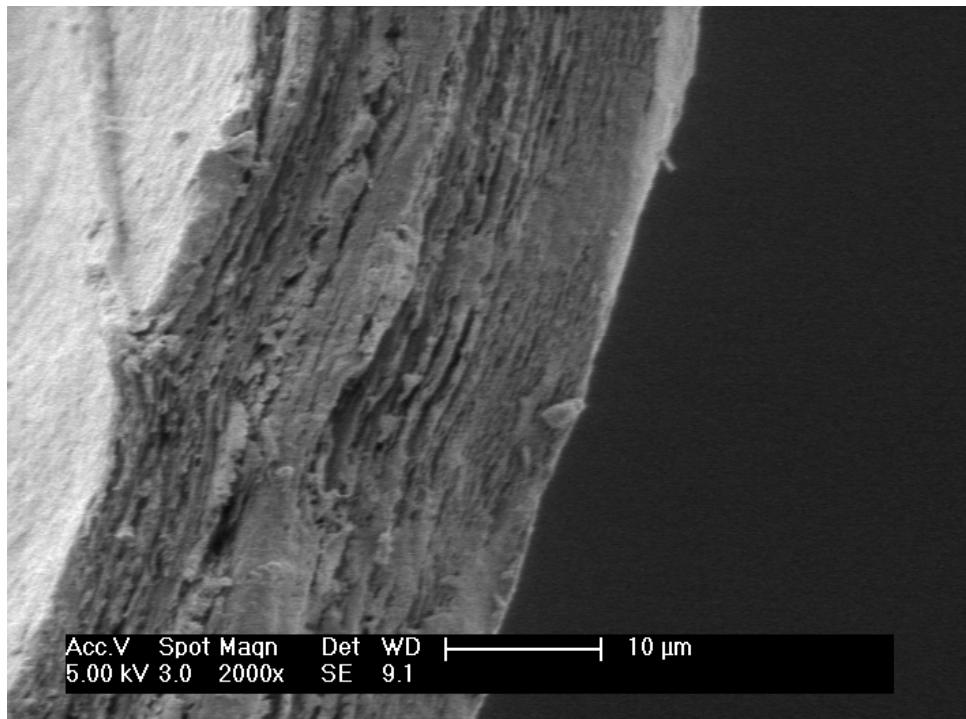


Figure 4

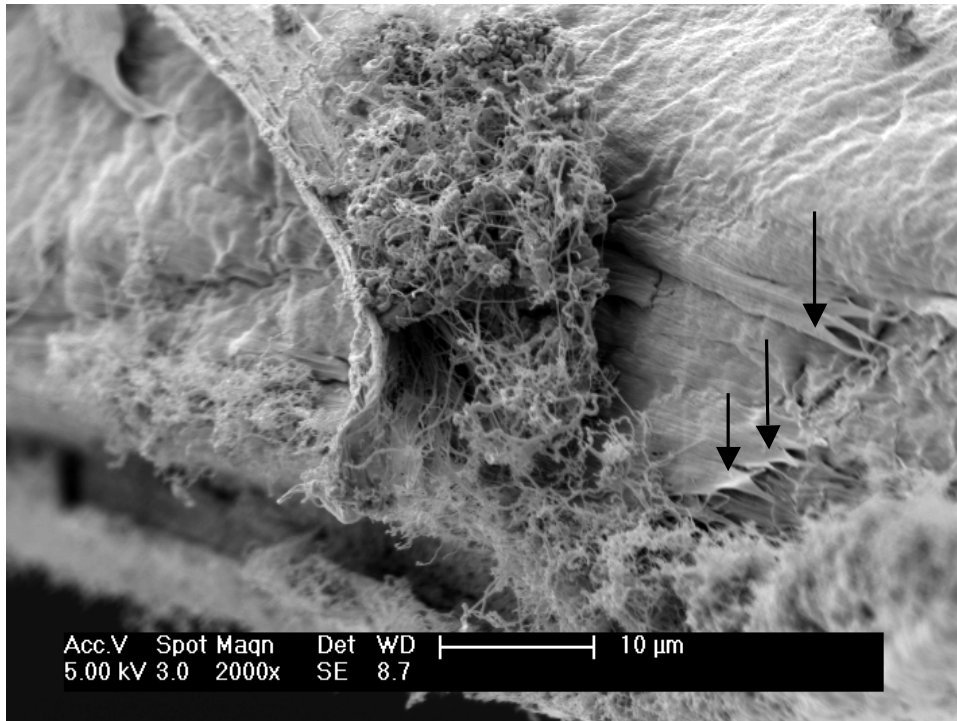
(a)



(b)



(c)



(d)

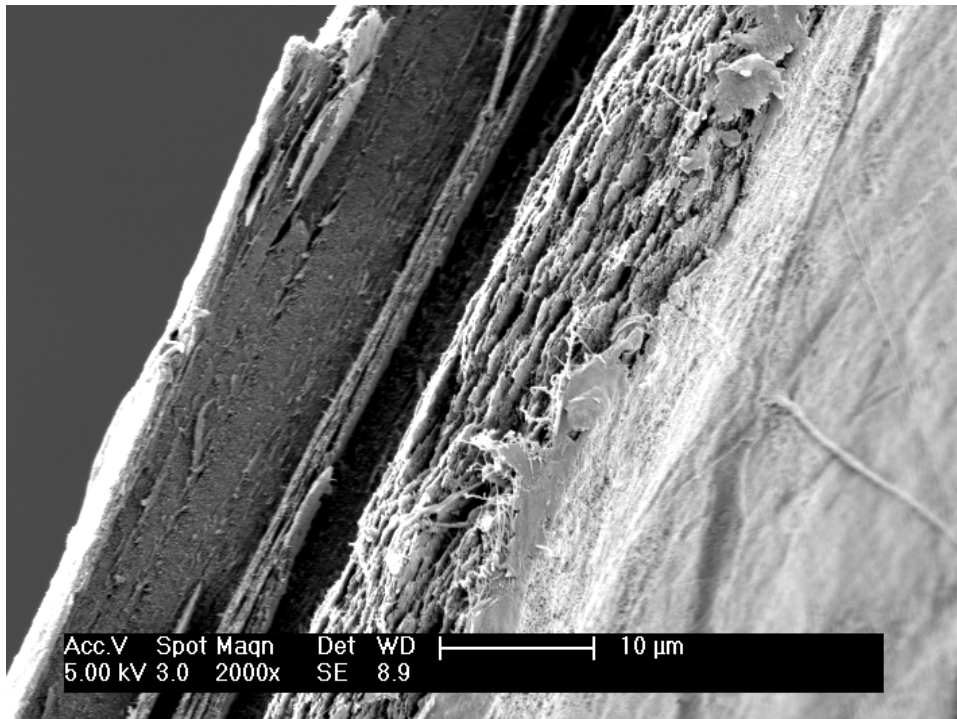


Figure 5

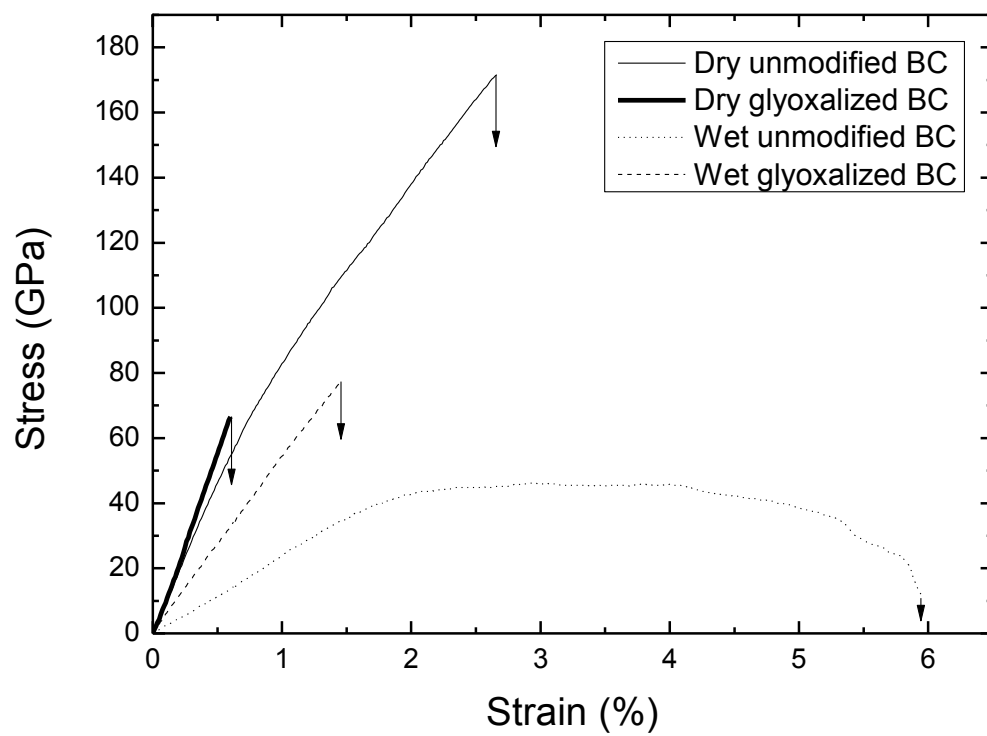
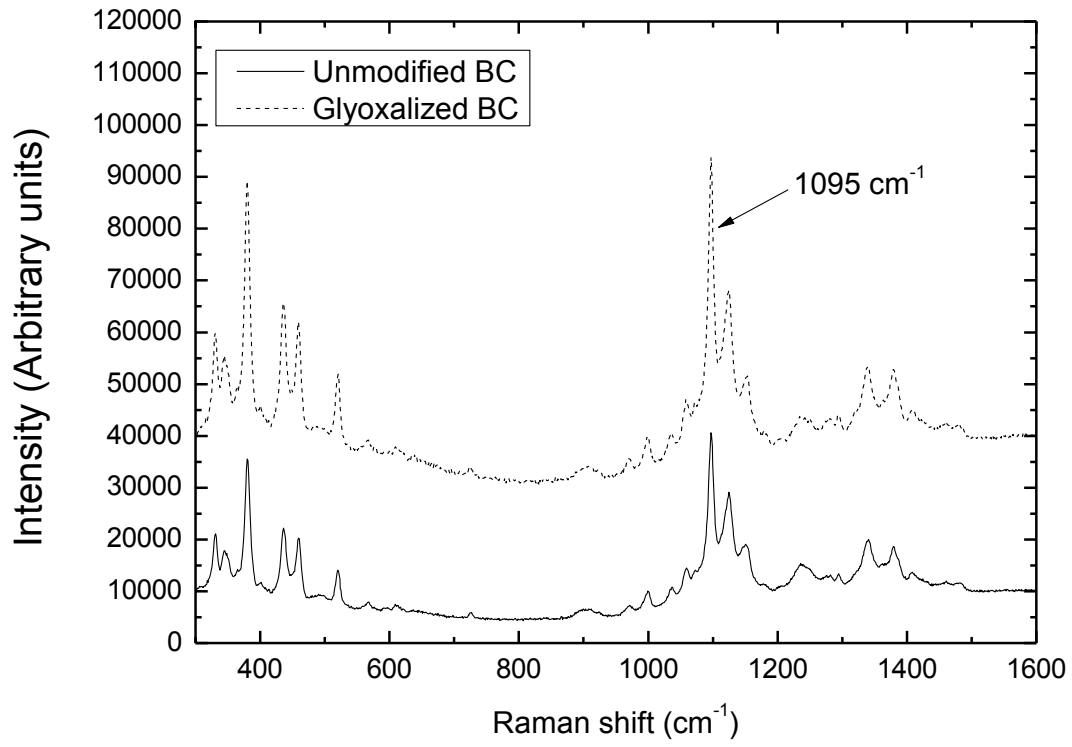
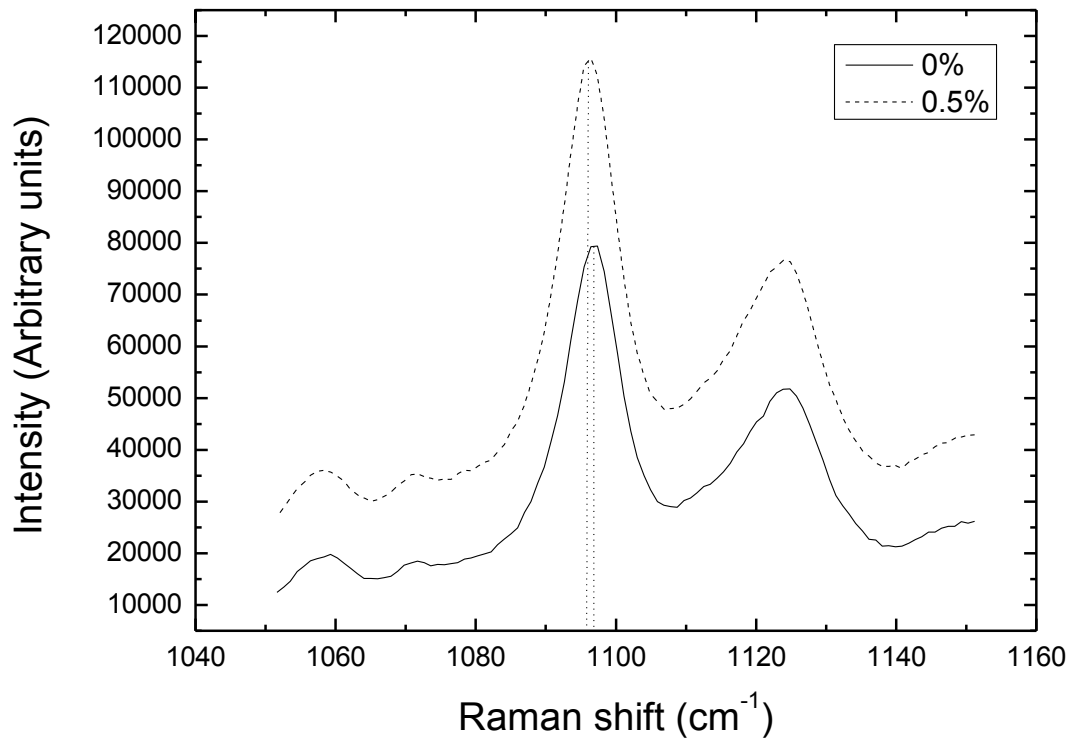


Figure 6

(a)



(b)



(c)

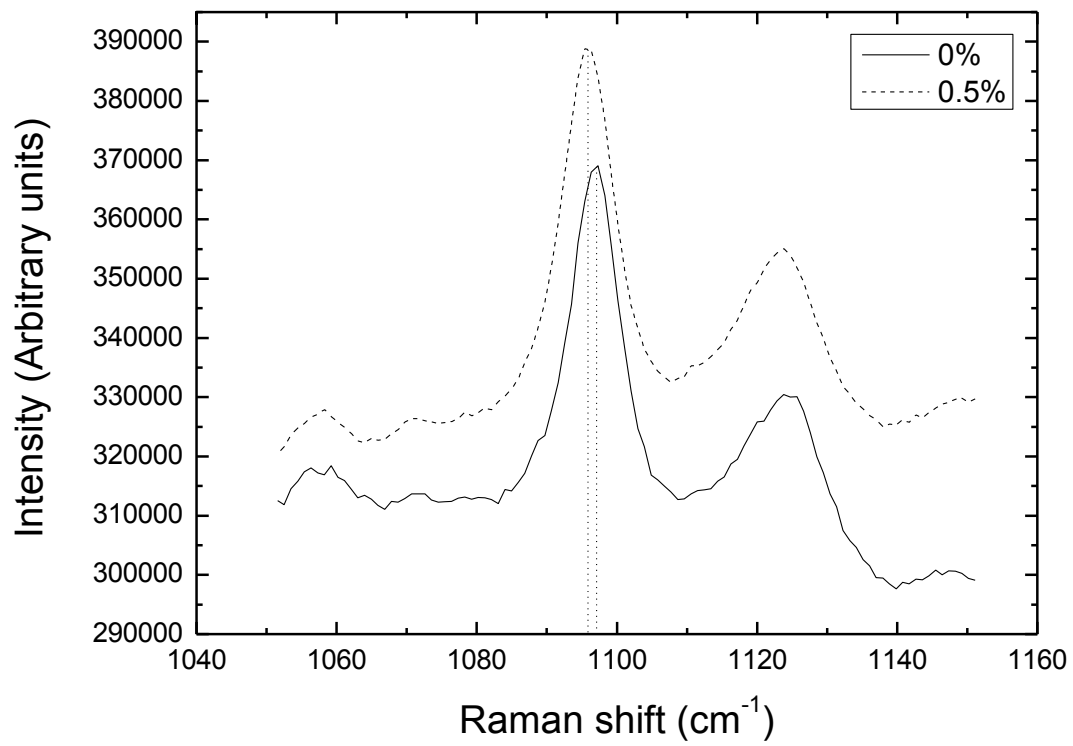
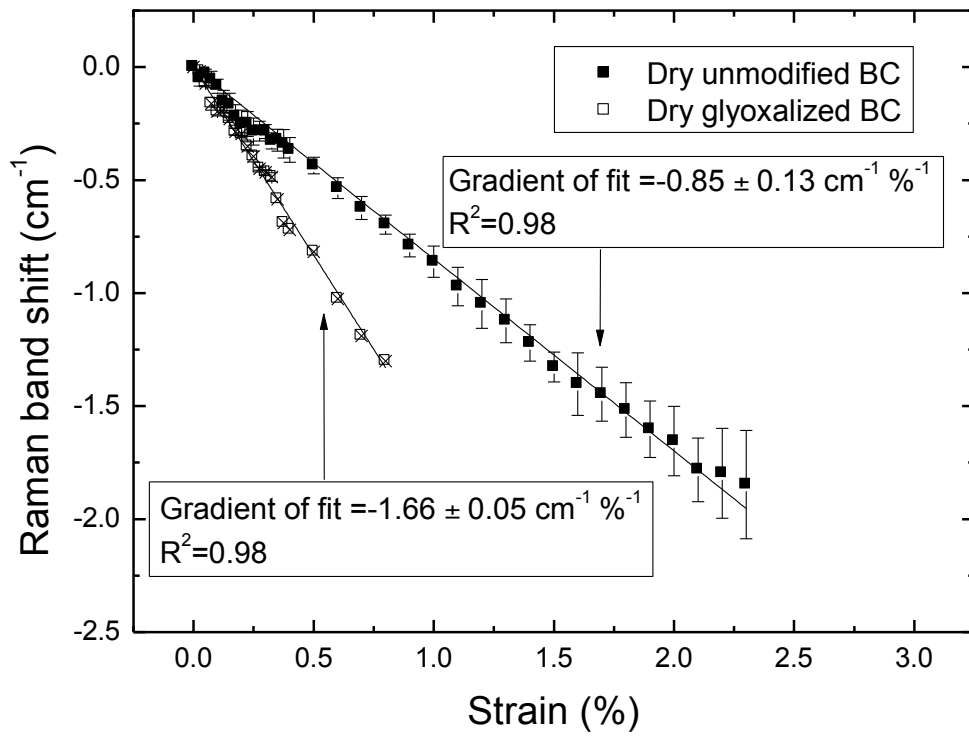


Figure 7

(a)



(b)

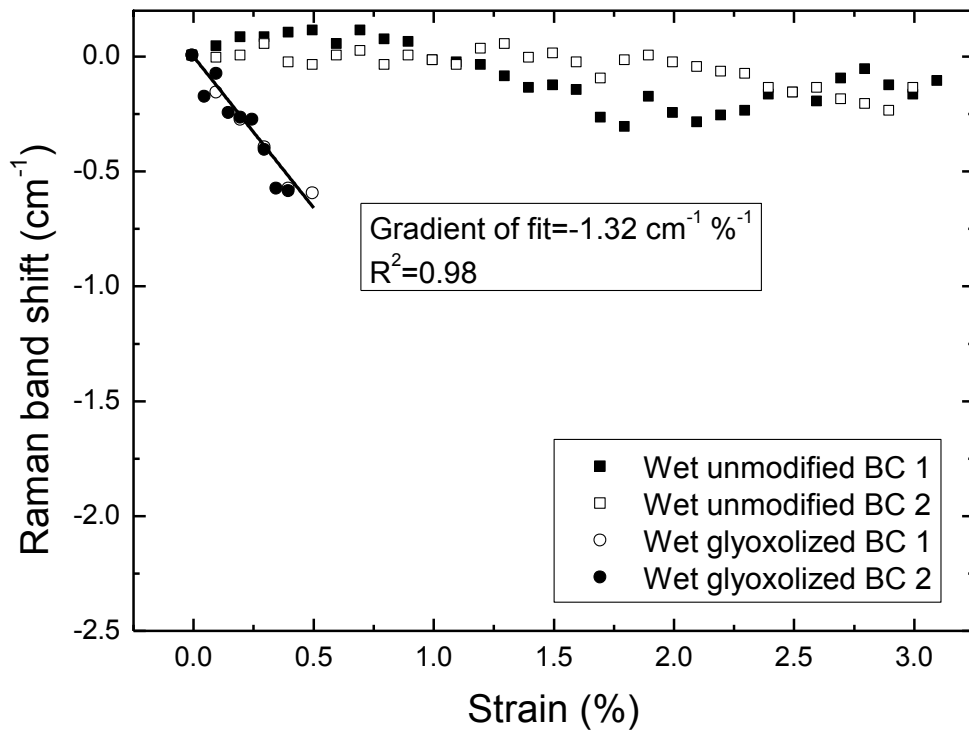


Figure 8